Characterization of the effects that play a role in photonic strain sensors in silicon-on-insulator technology

W.J. Westerveld[1,2], J. Pozo[2], P.J. Harmsma[2], R. Schmits[2], E. Tabak[2], S.M. Leinders[3], K.W.A. van Dongen[3], H. P. Urbach[1], M. Yousefi[2]

[1] Optics Research Group, Faculty of Applied Sciences, Delft University of Technology, Lorentzweg 1, 2628 CJ Delft, The Netherlands
[2] TNO, Stieltjesweg 1, 2628 CK Delft, The Netherlands
[3] Laboratory of Acoustical Imaging and Sound Control, Faculty of Applied Sciences, Delft University of Technology, Lorentzweg 1, 2628 CJ Delft, The Netherlands

Recently there has been a growing interest in sensing by means of optical microring resonators in photonic integrated circuits (PIC) that are fabricated in silicon-on-insulator (SOI) technology. Taillaert et. al. proposed the use of a waveguide based ring resonator as a strain gauge. However, the strong lateral confinement of the light in SOI waveguides and its corresponding modal dispersion was not taken into account. We present experimental results and understanding of the effects of an applied strain in the effective index in a SOI-PIC. In addition, we also investigated the influence of the waveguide geometry.

Introduction

Integrated photonics based on silicon technology has gained large academic as well as industrial interest over the last decade. While the telecommunication industry was the main driver, recently there has been a growing interest in sensing applications. This is in line with a greener future based on smart technology, where processes are continuously monitored and adaptively steered such that lesser resources are required. The CMOS technology opens the possibility for mass fabrication of PICs.

Piezoresistive electronic strain gauges are frequently used in micromachined electromechanical systems (MEMS) [1], such as the deflection sensor depicted in Fig. 1a. Taillaert *et. al.* [2] proposed the use of a microring resonator as a strain gauge. The all-optical system is insensitive to electromagnetic interference, does not have the danger of initiating gas explosions with electric sparks, and allows for high speed readout.

Amemiya *et. al.* [3] reported on the effect of strain on SOI ring resonators. However, the strong lateral confinement of the light due to the high refractive index contrast in SOI waveguides and its corresponding modal dispersion was not taken into account. We present experimental results and understanding of the effects of an applied strain S in the effective index n_e in a SOI-PIC.

Theory

In this section, we describe the effects that play a role when strain is applied to a ring resonator that has a racetrack-like shape with circumference l. Light is coupled from a connecting waveguide to the racetrack waveguide by means of a multimode interference (MMI) coupler. Having such a long racetrack allows us to neglect the effect of the bends

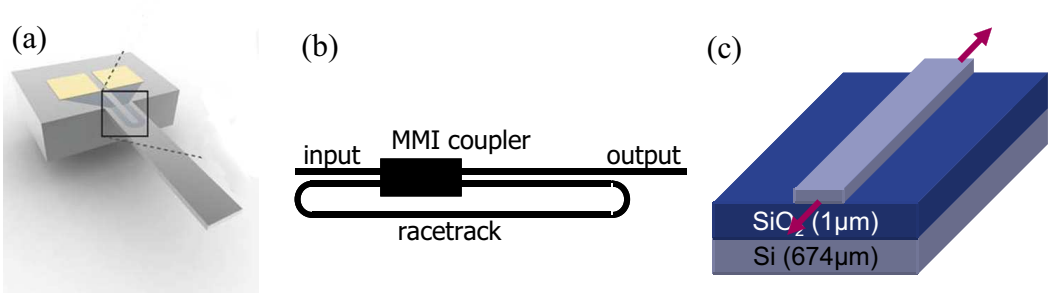

Figure 1: (a) Sketch of a cantilever with a traditional piezoresistive strain sensor, from [1]. (b) Sketch of the racetrack resonator. (c) Sketch of the waveguide of which the racetrack consists, with elongation indicated by the arrows.

and of the coupler. Transmitted spectrum at the output port of the connecting waveguide shows dips at the wavelengths λ_m of the resonances m of the racetrack, given by:

$$m \cdot \lambda_m = n_e(\lambda_m, S) \cdot l(S). \tag{1}$$

The effective index depends on the wavelength due to modal dispersion. We apply strain S in the longitudinal direction of the racetrack which shifts these resonance wavelengths. Three physical effects play a role when elongating the racetrack. First, the circumference of the racetrack is elongated. Second, the shape of the cross-section of the waveguide is shrunk due to Poisson's effect. Third, the refractive index of the silicon itself is changed due to the photo-elastic effect. The latter two effects manifest themself together in the effective index. The circumference $l = l_0(1+S)$, where l_0 is the circumference of the unstrained racetrack. Taking the partial derrivative of Eq. (1) to strain S gives:

$$m\frac{\partial \lambda_m}{\partial S} = \frac{\partial n_e}{\partial S} l + \frac{\partial n_e}{\partial \lambda_m}\frac{\partial \lambda_m}{\partial S} l + n_e \frac{\partial l}{\partial S}. \tag{2}$$

Rearranging this equation, substituting m from Eq. (1) at zero strain, substituting $\partial l/\partial S = l_0$, gives the linear influence of strain:

$$\frac{\partial \lambda_m}{\partial S} = \underbrace{\frac{n_e}{n_g}}_{\text{dispersion}} \left(\underbrace{\lambda_0}_{\text{circumference}} + \underbrace{\frac{\lambda_0}{n_e}\frac{\partial n_e}{\partial S}}_{\text{index}} \right), \tag{3}$$

where we recognize the effective group index $n_g \equiv n_e - \lambda(\partial n_e/\partial\lambda)$. The influences of modal dispersion, change in circumference and change in effective index are indicated.

Characterization method

The goal of this paper is to characterize the different terms in Eq. (3). We measure the net shift $\partial\lambda_m/\partial S$. The effective index n_e and the group index n_g are calculated with a mode solver (FMM method in the FimmWave software). This allows us to calculate the influence of strain on the effective index of the waveguide, $\partial n_e/\partial S$. For the stain measurements we fabricated a novel mechanical setup (Fig. 2) in which elastic bends are

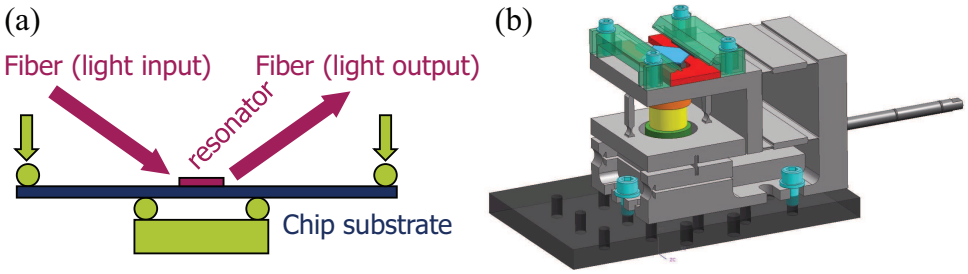

Figure 2: Tool for applying strain. (a) Sketch (side-view) of the mechanics. Equal forces are applied at the positions of the big arrows. Circles are the mechanical support bars. (b) CAD drawing.

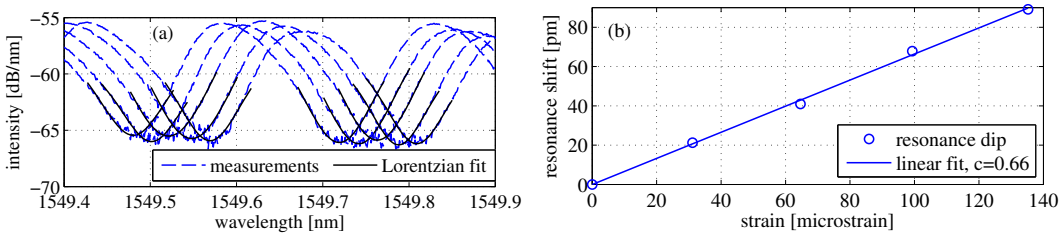

Figure 3: Measurement of resonance shift. (a) Five measured spectra with different strains. (b) Resonance wavelength of the left dip of (a) plotted versus strain.

used to provide a uniform strain in the region between the two middle supports, where the microresonator is placed. For each measurement, five transmission spectra are measured with strain varying from 0 to 140 microstrain ($\mu\varepsilon$), as shown in Fig. 3a. The position of the resonance dips are found by fitting Lorenzian distribution. Figure 3b shows the resonance wavelength versus strain, where $\partial\lambda_m/\partial S$ is obtained with a linear fit. Noise gives an error in the measured resonance wavelength, see (a), therefore we take the mean shift of a large number of resonances and estimate the error as the standard deviation of the random dip-to-dip variation. The error in the effective indices is neglected, which is supported by excellent agreement of the simulated and measured group index.

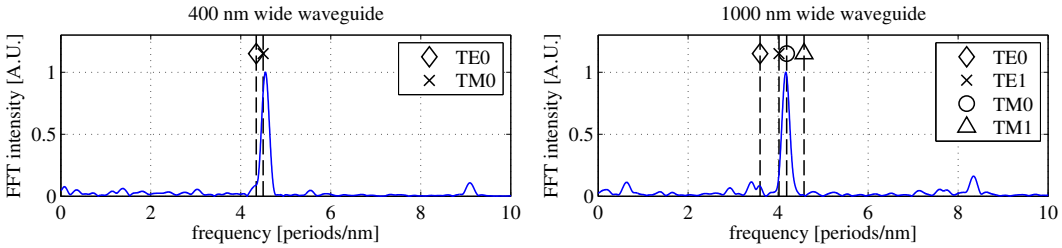

Figure 4: Fourier-transforms of the spectra of the zero-strain measurements. The $(\text{FSR})^{-1}$ corresponding to the group indices n_g as calculated with a mode solver are indicated.

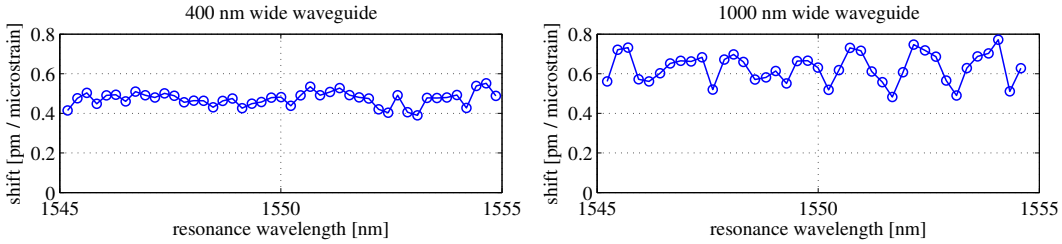

Figure 5: Measured shift of the resonance wavelengths due to applied strain.

Results

We fabricated two long racetrack resonators (length 1040 μm , radius 25 μm), oriented in the [110] crystalline direction, in a 300 nm high silicon guiding layer, with widths of 400 nm and 1000 nm. We excited the fundamental TM mode in the racetrack, which is verified by considering the Fourier-transform the measured spectrum. The reciprocal free-spectral-range, $(\mathrm{FSR})^{-1} = n_g \cdot l/\lambda_0$ corresponds to the group index of the modes. In Fig. 4 can be seen that the measurements agree excellently with the simulated group index of the fundamental TM-like mode in the waveguide.
Figure 5 presents the strain-induced shifts of all the resonances of the racetrack. The resonance-to-resonance variation is interpreted as the error in the measurement. From these measurements, we calculate the different effects that play a role (also see Eq. 3), and present them in the table below. Modal dispersion reduces the shift by a factor of 2, and the strain-induced effective index change contributes to $\sim$1/3rd of the net resonance shift.

Waveguide width [nm]	Measured shift [pm/$\mu\varepsilon$]	Index change $\partial n_e/\partial S$ [-]	Dispersion contribution [-]	Length contribution [pm/$\mu\varepsilon$]	Index contribution [pm/$\mu\varepsilon$]
1000	0.63 ± 0.08	-0.69 ± 0.24	0.56	1.55	0.39
400	0.47 ± 0.04	-0.73 ± 0.13	0.45	1.55	0.52

Conclusion

We demonstrated that strain can be measured with integrated optical racetrack resonators. When considering the shift of the optical resonance wavelength, the following effects play an important role: elongation of the racetrack length, modal dispersion of the waveguide, and the strain-induced change in effective refractive index.

References

[1] A.A. Barlian, W.-T. Park, J.R. Mallon, Jr., A.J. Rastegar, B.L. Pruitt, 'Review: Semiconductor Piezoresistance for Microsystems", in proc. of the IEEE **97**, 513 (2009).

[2] D. Taillaert, W. Van Paepegem, J. Vlekken, R. Baets, "A thin foil optical strain gage based on silicon-on-insulator microresonators", in proc. of SPIE **6619**, EWOFS 2007, Italy, 661914 (2007).

[3] [4] Y. Amemiya, Y. Tanushi, T. Tokunaga, S. Yokoyama, "Photoelastic Effect in Silicon Ring Resonators", Jpn. J. Appl. Phys. **47**, 2910 (2008).